

REPORT DOCUMENTATION PAGE

Form Approved
OMB No. 0704-0188

Public reporting burden for this collection of information is estimated to average 1 hour per response, including the time for reviewing instructions, searching existing data sources, gathering and maintaining the data needed, and completing and reviewing the collection of information. Send comments regarding this burden estimate or any other aspect of this collection of information, including suggestions for reducing this burden, to Washington Headquarters Services, Directorate for Information Operations and Reports, 1215 Jefferson Davis Highway, Suite 1204, Arlington, VA 22202-4302, and to the Office of Management and Budget, Paperwork Reduction Project (0704-0188), Washington, DC 20503.

1. AGENCY USE ONLY (Leave blank)		2. REPORT DATE 15 March 95	3. REPORT TYPE AND DATES COVERED Final - 15 June 94 - 15 March 95
4. TITLE AND SUBTITLE Infrared Detection of Chemical Corrosion on Metal Surface		5. FUNDING NUMBERS F49620-94-C-0033 3005/SS	
6. AUTHOR(S) Qing Dai, Andrew Freedman and Gary N. Robinson		65502F	
7. PERFORMING ORGANIZATION NAME(S) AND ADDRESS(ES) Aerodyne Research, Inc. 45 Manning Road Billerica, MA 01821		8. PERFORMING ORGANIZATION REPORT NUMBER AFOSR-TR-95-0267 ARI-RR-1117	
9. SPONSORING/MONITORING AGENCY NAME(S) AND ADDRESS(ES) Air Force Office of Scientific Research Bolling AFB, DC CAPT DeLong		10. SPONSORING/MONITORING AGENCY REPORT NUMBER NL DTIC SELECTED JUN 19 1995	
11. SUPPLEMENTARY NOTES This document has been approved for public release and sale; its distribution is unlimited. **		12b. DISTRIBUTION CODE	
12a. DISTRIBUTION/AVAILABILITY STATEMENT Unlimited Approved for public release; distribution unlimited.		12b. DISTRIBUTION CODE	

ABSTRACT (Maximum 200 words)

The sulfuric acid-induced corrosion of smooth (20 Å average roughness) aluminum surfaces has been studied in real time using an *in situ* Fourier transform infrared reflection absorption spectrometer (IRAS) and a quartz crystal microbalance. Submicron-thick, 35 - 55 wt% (5-12 molal), sulfuric acid films were formed on room temperature metal surfaces by the reaction of gas phase SO₃ and H₂O vapor in a flowing gas system at a total pressure of ~200 Torr. Using changes in spectral features that are linked to the production of Al³⁺ as indicators of corrosion, we conclude the rate of corrosion of the metal is strongly enhanced by both higher relative humidities and increased rates of sulfuric acid deposition. Ex situ IRAS measurements on aluminum foils indicated that this technique is suitable for the detection of corrosion on metal surfaces.

DTIC QUALITY INSPECTED 5

14. SUBJECT TERMS corrosion, sulfuric acid, aluminum, infrared, reflection-absorption spectroscopy		15. NUMBER OF PAGES 35	
		16. PRICE CODE	
17. SECURITY CLASSIFICATION OF REPORT UNCLASSIFIED	18. SECURITY CLASSIFICATION OF THIS PAGE UNCLASSIFIED	19. SECURITY CLASSIFICATION OF ABSTRACT UNCLASSIFIED	20. LIMITATION OF ABSTRACT SAR

NSN 7540-01-280-5500

Standard Form 298 (Rev. 2-89)
Prescribed by ANSI Std. Z39-18
298-102

19950615 054

**INFRARED DETECTION OF CHEMICAL
CORROSION ON METAL SURFACES**

Prepared by

Qing Dai , Andrew Freedman, and Gary N. Robinson
Aerodyne Research, Inc.
45 Manning Road
Billerica, MA 01821

Final Report
Contract No. F49620-94-C-0033

March 1995

TABLE OF CONTENTS

<u>Section</u>	<u>Page</u>
1. INTRODUCTION	1
1.1 Overview	1
1.2 Technical Background	2
1.3 References	4
2. SULFURIC ACID-INDUCED CORROSION OF ALUMINUM SURFACES	6
2.1 Introduction	6
2.2 Experimental	7
2.3 Results	9
2.3.1 Surface Chemistry	10
2.4 Corrosion Rate	16
2.4.1 Humidity Influence	16
2.4.2 Dependence on Initial SO ₃ Partial Pressure	18
2.5 Discussion	20
2.6 Conclusions	24
2.7 Acknowledgments	24
2.8 References	24
3. EX SITU IRAS MEASUREMENTS ON CORRODED ALUMINUM SAMPLES ...	26
3.1 IRAS Measurements	26
3.2 X-ray Photoelectron Spectroscopy (XPS)	30
3.3 Atomic Force Microscopy	31
3.4 Discussion	32

Accession For		
NTIS	CRA&I	<input checked="" type="checkbox"/>
DTIC	TAB	<input type="checkbox"/>
Unannounced		<input type="checkbox"/>
Justification		
By		
Distribution /		
Availability Codes		
Dist	Avail and/or Special	
A-1		

1. INTRODUCTION

1.1 Overview

Atmospheric chemical corrosion constitutes a severe threat to the structural integrity of many materials. Metals are particularly vulnerable to corrosion under atmospheric conditions as a result of their ability to participate readily in electrochemical reactions. The early *in situ* detection of metal corrosion as well as the ability to predict under what conditions and to what extent such corrosion will occur could save the United States aircraft industry and Air Force tens of billions of dollars.¹ However, despite years of research, the mechanisms and rate constants of many corrosion reactions are still not accurately known. In addition, although a number of sophisticated techniques exist for monitoring corrosion induced structural degradation of metals (e.g., ultrasonics, eddy current scanning, and x-ray radiography), they are often difficult and/or expensive to use in the field to detect aircraft corrosion damage *in situ*. Another significant drawback of these techniques is that they can only discern differences between the physical properties of corroded versus uncorroded metal (e.g., density, morphology, and electrical conductivity). As a result, their findings are sometimes subject to misinterpretation.

The objective of this project is to develop a versatile, inexpensive, and portable spectroscopic probe to quantify the atmospheric corrosion of metal surfaces on aircraft. Since many metals form insoluble salts as products of corrosion reactions, it should be possible to monitor the extent of metal corrosion by measuring the surface coverage of these products. For example, aluminum, which is a major component of aircraft, reacts with sulfate ions in acidic solutions to form insoluble aluminum hydroxysulfates. These compounds have distinctive infrared absorptions which can be monitored using infrared reflection absorption spectroscopy (IRAS). IRAS, which involves bouncing an infrared beam off of a reflective surface, is a highly sensitive nondestructive analytical technique for identifying and quantifying adsorbates on metal surfaces.^{2,3} It is capable of providing *in situ* information about the composition of the top few molecular layers of a surface in liquid or gaseous environments with submonolayer sensitivity. IRAS is potentially a much more powerful and versatile technique than those mentioned above since it can unambiguously detect actual corrosion products at monolayer to monolayer coverage. Furthermore, IRAS measurements can be performed with portable, field-ready Fourier transform infrared (FTIR) spectrometers, many of which are lightweight and cost less than \$50,000. Thus, IRAS can serve as a relatively inexpensive depot-level technique for detection of *in situ* aircraft corrosion.

As we will discuss below, we have been able to demonstrate the detection of sulfate-induced corrosion in an aluminum substrate on a 50-100 Å depth scale. For instance, Figure 1, shown below, provides the IRAS signature of a piece of aluminum foil which has been exposed to sulfate containing solution (at pH=3.5) at high relative humidity at 38 ° C for two days (a reasonable scenario for an airplane which is based in a hot humid urban or suburban environment). Note the large spectral features which are readily identifiable as linked to the corrosion process.

1.2 Technical Background

The corrosion of aluminum and most other metals under atmospheric conditions follows a sequence of physico-chemical events (Figure 2). First, reaction of the pristine aluminum surface with oxygen and/or water leads to the formation of a chemisorbed oxide layer. In a dry environment at ambient temperatures, this oxide layer is relatively inert and serves as a protective coating for the underlying metal. However, in the presence of ambient water vapor at 20° C, 10 to 30 layers of water molecules condense on the surface at relative humidities above 50%.^{4,5} In

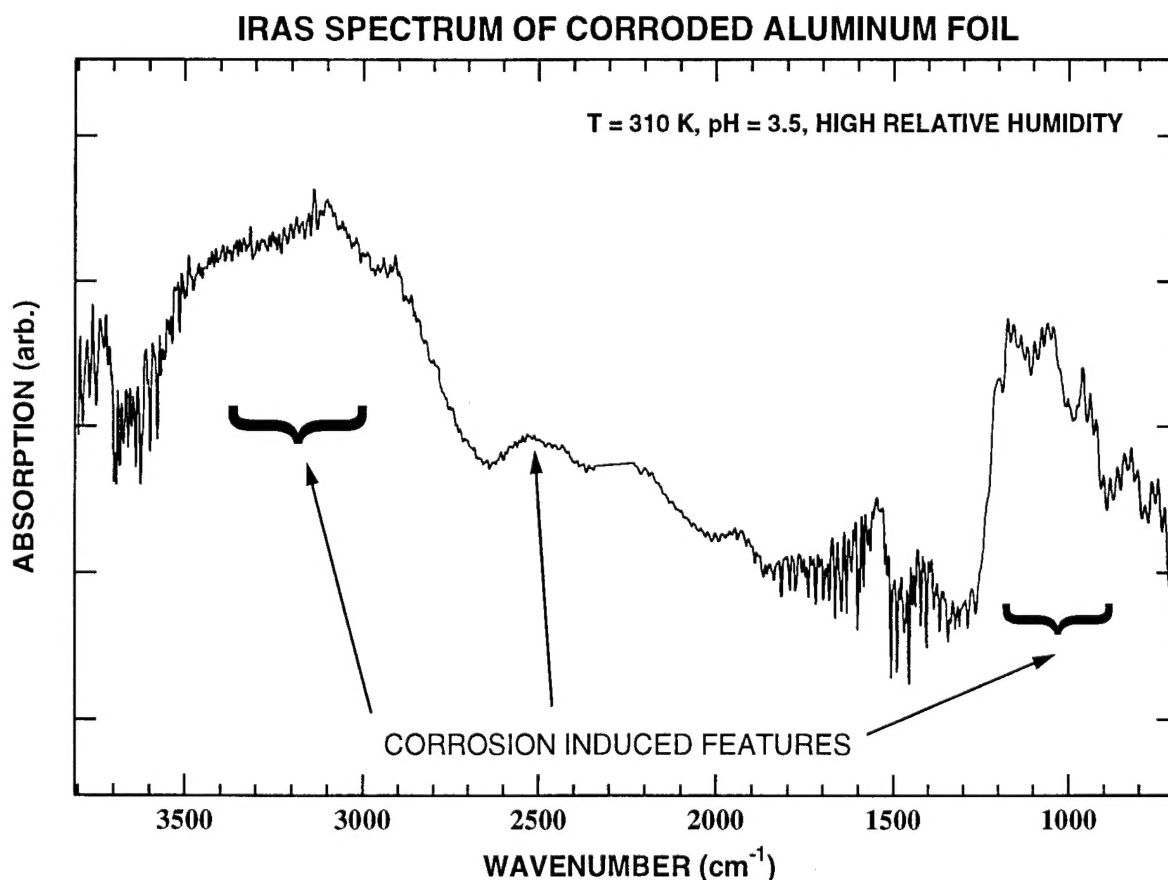


Figure 1. IRAS spectrum of a corroded piece of aluminum which has been exposed to sulfate solution at pH=3.5, then kept at high relative humidity at 38 °C for two days.

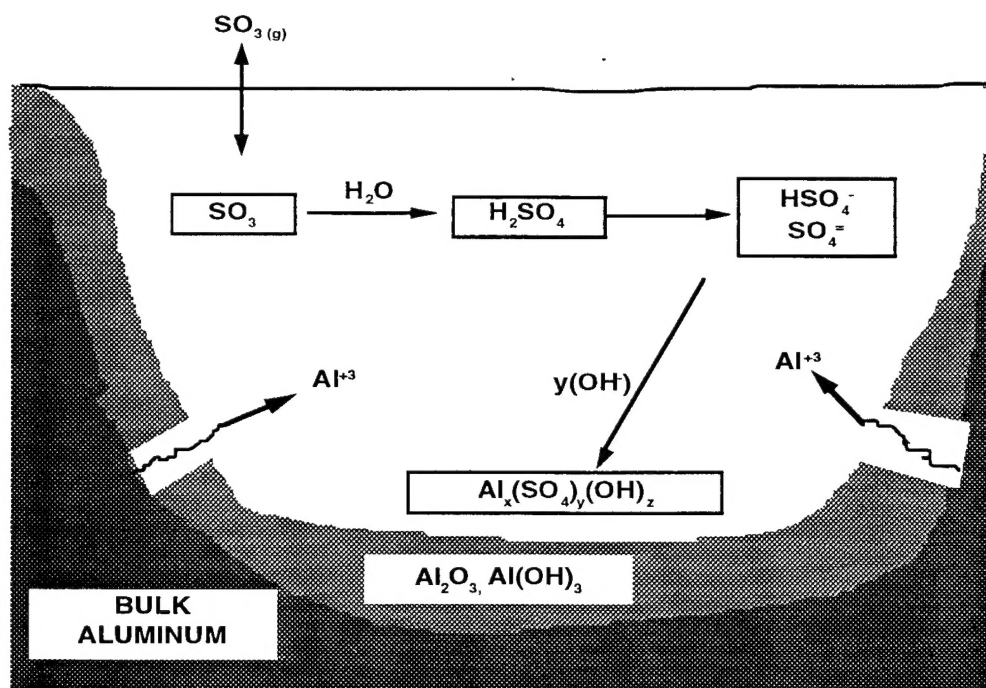
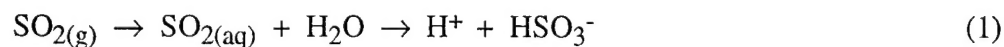


Figure 2. Schematic representation of the sulfur chemistry involved in the atmospheric corrosion of aluminum. Species in boxes have been confirmed by field measurements. (Adapted from Ref. 4.)

polluted industrial atmospheres, SO_2 dissolves in the surface water film whereupon reaction with dissolved hydrogen peroxide or ozone from the ambient atmosphere produces sulfuric acid:⁶



Alternatively, acidic rain or dew can deposit on the metal surface. Dissolution of the oxide in the resulting acidic solution enables Al^{3+} ions to enter the solution where they react with sulfates and water to form amorphous aluminum hydroxysulfates (of variable stoichiometry). These compounds will precipitate when the solution becomes supersaturated.^{4,7} In marine environments, chloride ions are present in the aqueous surface film and these will lead to the formation of a variety of aluminum hydroxychloride precipitates. Although field experiments have confirmed that these salts are formed during the atmospheric corrosion of aluminum^{8,9} and attempts have been

made to calculate thermochemical parameters for these compounds,¹⁰ the mechanisms and rate constants for these reactions are uncertain.

Naturally occurring aluminum salts exist whose infrared spectra have been measured.¹¹ Although, these compounds have different stoichiometries from the amorphous salts formed during aluminum corrosion, their infrared spectra should not differ dramatically from those of the corrosion salts and we should therefore be able to use these spectra to identify the corrosion salts on the aluminum surface. With FT-IRAS it is possible to measure fractional absorbances on the order of 10^{-3} - 10^{-4} which translates into detection sensitivities of 1 - 10 monolayers for adsorbates with moderately strong absorption coefficients. Hydrated Al^{3+} ions also have distinctive IR absorptions^{12,13} so spectra of aqueous films on aluminum surfaces can be used to monitor corrosion as well as spectra of the precipitates. It should be noted that FT-IRAS has already been used in the laboratory to observe the corrosion of copper by sulfur dioxide¹⁴ and the electrochemical etching of aluminum in acid chloride solutions.¹⁵

We have conducted a number of in situ and ex situ studies in order to demonstrate the power of IRAS to study the corrosion process, both as a tool to elucidate the chemistry involved and to act as a potential field monitor. Section 2 will present the contents of a paper which has been submitted to the Journal of the Electrochemical Society involving detailed chemistry of the sulfuric acid/aluminum corrosion system. Section 3 will present a description of a limited number of experiments involving ex situ measurements of corrosion.

1.3 References

1. Proceedings of the AFWAL/ML Workshop on Nondestructive Evaluation of Aircraft Corrosion: Requirements and Opportunities for Research and Development, May 1983, J.A. Moyzis, Chairman; DTIC Report No. WL-TR-92-4095.
2. R.M. Crooks, C. Xu, L. Sun, S.L. Hill, and A.J. Ricco Spectroscopy 8(7), 28 (1993).
3. J. Pritchard, Chemical Physics of Solids and their Surfaces, Vol. 7, M.W. Roberts and J.M. Thomas, eds. (Chemical Society, London, 1977).
4. T.E. Graedel, J. Electrochem. Soc. 136, 204C-212C (1989).
5. P.B.P. Phipps and D.W. Rice, in Corrosion Chemistry, G.R. Brubaker and P.B.P. Phipps, eds., Am. Chem. Soc. Symp. Ser. 89, 235-261 (1979).
6. R.P. Wayne, Chemistry of Atmospheres, 2nd ed. (Oxford, 1991), p. 244.
7. T.E. Graedel, Mat. Res. Soc. Symp. Proc. 125, 95-105 (1988).

8. J.J. Friel, Corrosion **42**, 422 (1986).
9. H. Bassett and T.H. Goodwin, J. Chem. Soc. 2239 (1949).
10. R.T. Foley and T.H. Nguyen, J. Electrochem. Soc. **129**, 464-467 (1982).
11. H. Moselhy, V. Izvekov, G. Pokol, T. Gal, S. Gal, and E. Pungor, Magy. Kem. Foly. **98**, 459-462 (1992).
12. J.F. McIntyre, R.T. Foley, and B.F. Brown, Appl. Spectrosc. **36**, 128-136 (1982).
13. J.J. Fripiat, F. Van Caulwelaert, and H. Bosmans, J. Phys. Chem. **69**, 2458-2461 (1965).
14. D. Persson and C. Leygraf, J. Electrochem. Soc. **140**, 1256-1260 (1993).
15. C. F. Lin, K.R. Hebert, and M.D. Porter, Proc. -Electrochem. Soc. **92-9**, 240-252 (1992).

2. SULFURIC ACID-INDUCED CORROSION OF ALUMINUM SURFACES

The sulfuric acid-induced corrosion of smooth (20 Å average roughness) aluminum surfaces has been studied in real time using an *in situ* Fourier transform infrared reflection absorption spectrometer and a quartz crystal microbalance. Submicron-thick, 35 - 55 wt% (5-12 molal), sulfuric acid films were formed on room temperature metal surfaces by the reaction of gas phase SO₃ and H₂O vapor in a flowing gas system at a total pressure of ~200 Torr. The deposition of the acid films and subsequent changes in their chemical composition could be monitored using characteristic infrared absorption features. The corrosion process always significantly perturbed the spectral signature of the films from that which was observed on inert gold surfaces. Using changes in spectral features that are linked to the production of Al³⁺ as indicators of corrosion, we conclude the rate of corrosion of the metal is strongly enhanced by both higher relative humidities and increased rates of sulfuric acid deposition. *Ex situ* atomic force microscopy analysis of the post-exposure Al samples indicates that 200 Å thick layers of precipitates are present on the surface.

2.1 Introduction

The deposition and/or formation of sulfuric acid on aluminum surfaces is probably the major cause of atmospheric corrosion of structural aluminum in urban and industrial environments.^{1,2} The corrosion process follows a sequence of complex physico-chemical events.^{3,4} First, reaction of the pristine metal surface with oxygen and/or water leads to the formation of a chemisorbed oxide layer. In a dry environment at ambient temperatures, this oxide layer is relatively inert and serves as a protective coating for the underlying metal. In polluted industrial or urban atmospheres, sulfur dioxide, SO₂, dissolves in the surface water film whereupon reaction with dissolved hydrogen peroxide or ozone from the ambient atmosphere produces sulfuric acid.⁵ Alternatively, acidic rain or dew can deposit on the metal surface. Dissolution of the oxide in the resulting acidic solution (at pH < 4) leads to the acid-promoted oxidation of aluminum metal. The Al³⁺ ions produced by the oxidation process enter solution and react with sulfates and water to form aluminum sulfate and/or hydroxysulfate salts of variable stoichiometry. These compounds will precipitate when the solution becomes supersaturated. Although field experiments have confirmed that these salts are formed during the atmospheric corrosion of aluminum^{6,7} and attempts have been made to calculate thermochemical parameters for these compounds,⁸ the mechanisms and kinetics of the underlying reactions are uncertain.

In order to elucidate the chemistry underlying the corrosion of aluminum surfaces, we have conducted real time experiments using *in situ* Fourier transform infrared reflection absorption

spectroscopy (IRAS). With IRAS, reactants and products on a metallic surface can be detected by measuring the loss of reflected light intensity due to absorption by adsorbed species.^{9,10,11} Although IRAS is routinely used by the surface science community for the study of interfacial processes, its application to the *in situ* study of atmospheric corrosion is surprisingly uncommon.¹² Using this technique, we have monitored changes in the chemical composition of adsorbed films of sulfuric acid on aluminum surfaces as a function of different experimental variables. We have also employed an *in situ* quartz crystal microbalance (QCM) to obtain information on the growth rate of the adsorbed films and *ex situ* atomic force microscopy (AFM) to provide information about changes in surface morphology as a result of corrosion.

In these experiments, we proceeded by identifying the relevant spectral features of a growing film of sulfuric acid and its dissociation products (sulfate, bisulfate and hydronium ions) formed by gas phase reaction of sulfur trioxide, SO_3 , and water vapor in a flowing gas system at room temperature. In addition, we have identified a new spectral feature which is linked to the production of Al^{3+} , presumably a result of the dissolution of the protective oxide layer and subsequent corrosion of the underlying metal film. Using the changes in these features as quantitative indicators of corrosion, we have measured the relative corrosion rates of aluminum as a function of both humidity and sulfuric acid deposition rate. Semi-quantitative estimates indicate that the corrosion process is strongly enhanced by an increase in relative humidity. We note that the choice of directly forming sulfuric acid using sulfur trioxide was made in order to simplify the analysis of the results and to accelerate the corrosion process.

2.2 Experimental

All experiments described here were carried out in a 10 cm diameter stainless steel flow tube. The cell could be pumped out to a base pressure below 10^{-3} Torr using a mechanical pump with a liquid nitrogen trap to eliminate oil vapor backdiffusion. The metal samples were mounted on a manipulator located in the center of the tube. The distance of the sample from the gas inlet (15 cm), gas flow speeds ($\sim 2 \text{ cm sec}^{-1}$) and cell pressure (200 Torr) were chosen to ensure the presence of laminar gas flow conditions at the sample.¹³

Sulfuric acid films were formed on metal surfaces by the reaction of gas phase sulfur trioxide and water vapor. H_2O and SO_3 were introduced into the flow tube using nitrogen as a carrier gas with a total gas flow of $\sim 2300 \text{ sccm}$. The water vapor flow was produced by bubbling nitrogen through liquid water whose temperature was adjusted to produce the desired partial pressure in the flow tube. In high humidity experiments, the H_2O partial pressure in the flow tube, $P_{\text{H}_2\text{O}}$, was maintained at $\sim 16 \text{ Torr}$ [80% relative humidity (RH)], while in the low humidity

experiments, $P_{H_2O} \approx 6$ Torr (30% RH). The water inlet line was heated to prevent any condensation of H_2O , which would affect the water vapor pressure in the flow tube. Sulfur trioxide (Alfa) was redistilled and then purified using a number of freeze-thaw cycles. Its vapor was introduced into the chamber by flowing N_2 into a glass bulb containing SO_3 solid kept in an ice water bath. At 273K, the α and β forms of SO_3 (the most stable isomers) have vapor pressures of ~ 40 Torr.¹⁴ The SO_3/N_2 flow rate was adjusted in order to vary the SO_3 partial pressure in the chamber. The nominal SO_3 partial pressure investigated in these experiments ranged from 0.036 to 0.68 Torr.

The sulfuric acid films are probably caused by deposition of sulfuric acid droplets that form in the flow tube. We performed IR absorption experiments to monitor any chemical reactions that might occur in the gas phase (rather than on the Al sample) and did not observe any absorption features that may be related to gas phase SO_3 or H_2SO_4 with water vapor present. This indicates that the reaction of SO_3 with H_2O to form sulfuric acid and the subsequent condensation of acid droplets occur on a very fast time scale. This finding is supported by recent work by Kolb and co-workers¹⁶ which indicates that, under the conditions of our experiments, the gas phase reaction of SO_3 with water vapor is sufficiently fast to convert all of the SO_3 to sulfuric acid in a small fraction of the reactant residence time in the flow tube.

The aluminum samples studied here were prepared by vapor depositing 2000 Å of aluminum on polished Si single crystal (100) wafers. The surface roughness was ~ 20 Å as determined by atomic force microscopy (AFM) measurements. *Ex situ* X-ray photoelectron spectroscopy measurements indicated the presence of both aluminum oxide and metallic aluminum. Because the escape depth of the Al (2p) photoelectron is only on the order of 20-30 Å, the oxide layer cannot be much thicker than that. Gold surfaces, prepared by vapor depositing Au on Si wafers precoated with chromium, were studied as reference surfaces that are inert to attack by H_2SO_4 . We have also investigated the corrosion of Al foils (micron scale roughness) under H_2SO_4 exposure. No substantial differences from the vapor deposited Al results were observed and hence these results are not presented.

Infrared reflection absorption spectra were obtained by directing a modulated infrared beam from a Midac, M2400, FTIR spectrometer onto the metal samples at an incident angle of 75° off normal using beam focusing and steering mirrors. The beam size on the sample surface was approximately 5 x 15 mm². The reflection absorption spectra were recorded using a liquid nitrogen-cooled HgCdTe detector with a cutoff frequency of ~ 700 cm⁻¹. Optical access to the chamber was provided by a pair of KRS-5 (thallium bromoiodide) windows.

In addition, an *in situ* quartz crystal microbalance (QCM) was used to determine the time-dependent weight gain on the surfaces when exposed to H_2SO_4 . Quartz crystals coated with either Al or Au were used depending on which surface was being studied by IRAS. The microbalance was mounted about 3 cm below the samples on which IRAS studies were performed (which were at the center of the flow stream). The measured weight gain represented a lower limit to the true weight gain on the IRAS-probed surfaces because of the possibility of a radial concentration gradient of sulfuric acid in the flow tube caused by diffusion to and subsequent condensation onto the tube walls.¹⁵ However, the correlation of IR spectral features with weight gain measurements was quite reproducible.

Ex-situ atomic force microscopy (AFM) experiments were also performed in order to obtain morphological information about the clean and corroded Al surfaces. These images were obtained in contact mode at 30% RH with a home-made AFM in the laboratory of Dr. M. Salmeron at the Lawrence Berkeley Laboratory.

In a typical experiment, the chamber and sample were first exposed to water vapor until the QCM indicated that a stable water film had been established. Once the sample surface was saturated with H_2O , the SO_3 was introduced into the chamber. FTIR spectra and QCM measurements were then taken every 5-10 minutes during the exposure to both gases, for a period of 240 minutes per experiment. All experiments were performed at room temperature (295 K).

Since the surface films that were investigated extended to as many as 1000 monolayers, a non-polarized IR beam was sufficiently sensitive for these studies. However, we were careful to ensure that what was observed was indeed from the sample rather than from anything else in the IR beam path. For instance, after the H_2O and SO_3 lines were shut off at the end of each experiment, the chamber was evacuated and purged with dry nitrogen for 30-60 minutes; IRAS spectra of the sample were then recorded. We also measured IR spectra without the KRS-5 windows in order to account for any contaminants condensed on the windows. In both cases, little change was observed in the IR spectra, indicating that the spectral features indeed resulted from corrosion processes on aluminum surfaces. On Au, however, all the features observed during H_2SO_4 exposure gradually disappeared after one or two hours of pumping under N_2 purging, indicating that only sulfuric acid was present on the surfaces.

2.3 Results

In this section, we will discuss the surface chemistry that occurs when sulfuric acid, formed from sulfur trioxide and water vapor, deposits on an aluminum surface. This includes the

adsorption and subsequent dissociation of the acid film and corrosion of the underlying metal. Data will be presented on the corrosion of aluminum films as a function of relative humidity and sulfur trioxide vapor concentrations.

2.3.1 Surface Chemistry

The growth of the adsorbed sulfuric acid films was studied by monitoring both the weight gain and infrared spectra of Al surfaces. Figure 1 presents the results of weight gain measurements on Al surfaces during water and sulfur trioxide exposure under various conditions. Curve (a) shows the weight gain when the sample was exposed to H₂O only at 80% relative humidity (RH) (~16 Torr at 295 K). Note that within 20 minutes the surface became saturated with about 60 Å or 20 monolayers of H₂O, in agreement with previous results.¹⁷

The weight gain increased dramatically once SO₃ was introduced into the chamber, as shown in Curves (b) and (c). The data in (b) were obtained at 80% RH and an initial SO₃ pressure of 0.036 Torr. More than 14 µg cm⁻² accumulated on the surface (~1400 Å assuming the bulk density of water). When conditions were further changed, as in (c) (P_{SO₃} = 0.18 Torr, 30% RH), the measured weight gain also changed. We also note that similar gains in weight were observed as a function of time on both Au and Al surfaces under the same experimental conditions. We will show below that, although the Al and Au surfaces displayed similar weight gains, their chemical reactivities differed substantially.

As mentioned above, IRAS spectra can provide both qualitative and quantitative information on the species being formed in the growing films as a function of reactant exposure. IRAS spectra of the Al samples measured during a 240 minute exposure to SO₃ and H₂O are shown in Figure 2. These spectra reflect the deposition of sulfuric acid and its subsequent dissociation and reaction with the Al substrate. The relative humidity during this experiment was kept at 80% and the SO₃ partial pressure was ~0.68 Torr. The IR spectrum of the H₂O-saturated surface was used as a reference for background subtraction. Spectrum (a), taken only several minutes after introduction of H₂O and SO₃, showed well defined absorption features at 1189 cm⁻¹, 1050 cm⁻¹, and 900 cm⁻¹. From Table 1, we can see that this IR spectrum is characteristic of liquid H₂SO₄.¹⁸

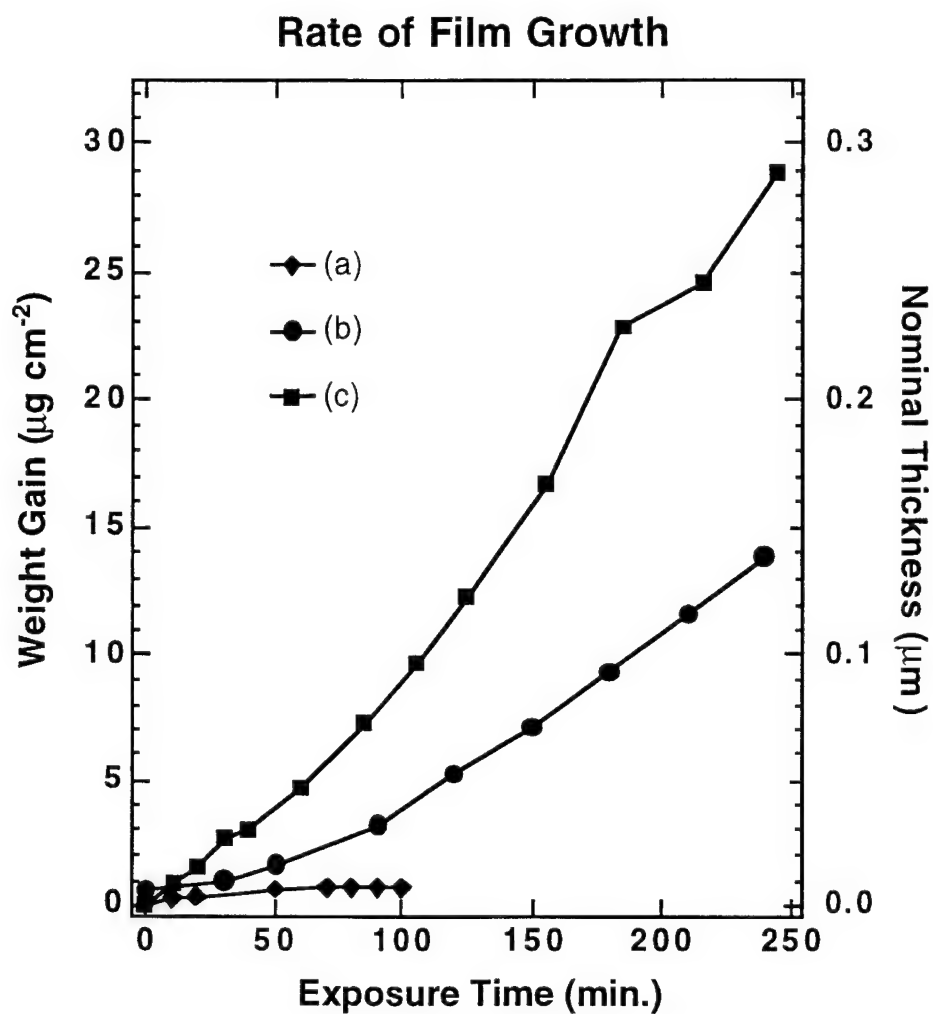


Figure 1. Weight gain on an Al film measured by a quartz crystal microbalance. (a): Weight gain due to water condensation. (b): Weight gain during H_2SO_4 exposure. $P = 0.036$ Torr, 80% relative humidity. (c): Weight gain for $P = 0.18$ Torr, 30% relative humidity.

Time Evolution of IR Spectra

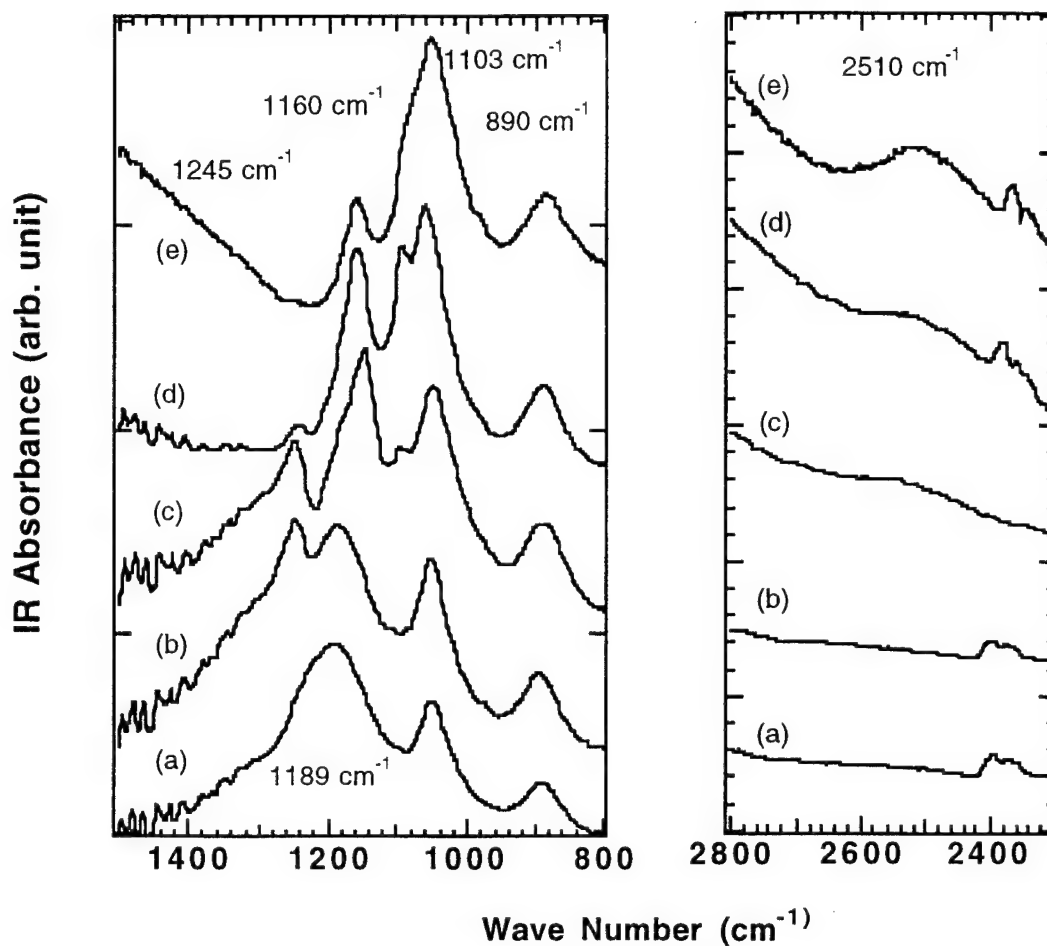


Figure 2. Time evolution of IRAS spectra of Al surfaces during H_2SO_4 exposure. $P = 0.68$ Torr, and 80% relative humidity. Exposure time: (a): 3 minutes; (b): 10 minutes; (c): 80 minutes; (d): 160 minutes; and (e) 240 minutes. The spectra remain the same as (e) after apparatus purge and evacuation. (The peaks at 2400 cm^{-1} are caused by incomplete subtraction of absorption by atmospheric carbon dioxide.)

Table 1 - Assignments of Observed Spectral Features

Spectral Features (cm ⁻¹)	Assignments	Literature Values ¹⁸
890	H ₂ SO ₄ , HSO ₄ ⁻	905, 885
1050	HSO ₄ ⁻	1050
1103-1096	SO ₄ ²⁻	1104
1150-1160	H ₃ O ⁺	1134
1189	H ₂ SO ₄	1190
1245	HSO ₄ ⁻	1230
~1340	HSO ₄ ⁻	1341
~2900	H ₂ SO ₄ (O-H)	
~3400	H ₂ O(O-H)	3445

In the absence of corrosion, the condensed sulfuric acid films in these experiments are in equilibrium with the gas phase water vapor. Since the equilibrium vapor pressures of SO₃ and H₂SO₄ over concentrated sulfuric acid are negligible at 295 K, the composition of the sulfuric acid film can thus be derived from the water vapor pressure in the cell and the substrate temperature. For the two partial pressures of water vapor used in these experiments, 16 and 6 Torr, one would expect the initial film composition to be 35 and 55 weight per cent sulfuric acid (roughly 5 and 12 molal) respectively.¹⁹ Zhang et al.²⁰ and Middlebrook et al.²¹ have measured the infrared spectra of thin H₂SO₄ films as a function of sulfuric acid concentration. They have determined that comparing the O-H stretch absorption intensities from H₂O and H₂SO₄ in the region of 3500 cm⁻¹ - 2800 cm⁻¹ provides a good estimate of the sulfuric acid concentration. We have performed a rough line shape analysis of spectra taken after 3 minutes exposure at both relative humidities. This analysis gave sulfuric acid concentrations of 39 and 58 weight per cent for 80% and 30% RH respectively. This result is in excellent agreement with the concentrations derived assuming equilibrium between the sulfuric acid film and the ambient water vapor. These results imply that, whereas the humidity and substrate temperature determine the composition of the acid, the initial SO₃ partial pressure influences the rate at which sulfur species, in the form of sulfuric acid, deposit on the surface.

After ten minutes of continuous exposure to water and sulfur trioxide, it was possible to observe the dissociation of sulfuric acid to bisulfate [Figure 2 (b)]. The major change in (b) is that the 1189 cm⁻¹ peak has split, giving a new peak at 1245 cm⁻¹. Based on earlier studies by Querry et al.,¹⁸ the 1245 cm⁻¹ peak is due to IR absorption from the bisulfate ion, HSO₄⁻. In Figure 2(c), recorded after 80 minutes total exposure, both HSO₄⁻ (1245 cm⁻¹) and H₂SO₄

(1189 cm^{-1}) have decreased in intensity, while two new peaks at 1150 cm^{-1} and 1103 cm^{-1} have appeared. The peak at $\sim 1150 \text{ cm}^{-1}$ is assigned to H_3O^+ and the 1103 cm^{-1} peak is assigned to SO_4^{2-} by Querry et al.¹⁸ and Zhang et al.²⁰ In short, we are observing the conversion of H_2SO_4 and HSO_4^- into SO_4^{2-} and H_3O^+ .

These changes became more prominent as the experiment progressed. After 160 minutes, as shown in Figure 2(d), the HSO_4^- peak (1245 cm^{-1}) and H_2SO_4 (1189 cm^{-1}) peaks have almost disappeared, and the SO_4^{2-} (1103 cm^{-1}) peak has grown significantly. Along with these changes, a new feature at 2510 cm^{-1} was also observed. This new peak grew with time, as shown in the right panel of Figure 2. This peak has been observed before by McIntyre et al. in $\text{Al}_2(\text{SO}_4)_3$ and other aluminum salt solutions, and was assigned to the symmetric O-H stretch in water coordinated to Al^{3+} .²² A detailed assignment of the spectral features is given in Table 1.

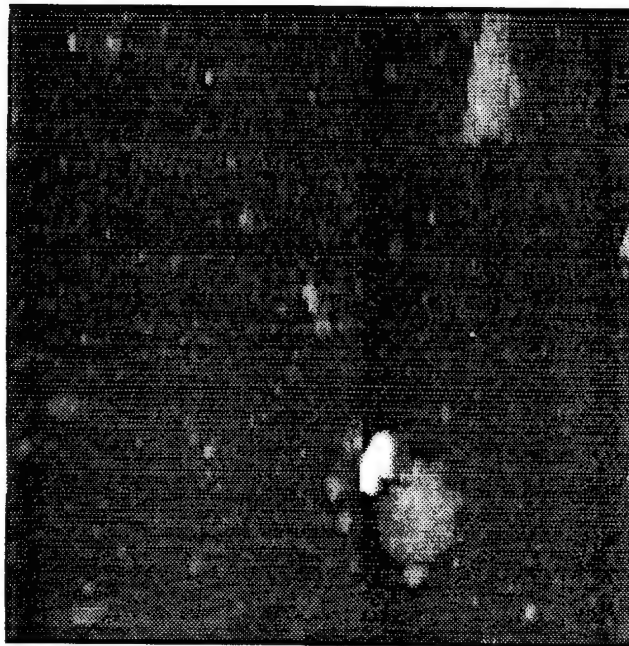
Based on these observations, we conclude that in the first few minutes of exposure to sulfur trioxide and water, a H_2SO_4 film deposits on the aluminum surface. H_2SO_4 reacts with the surface to form $\text{Al}(\text{H}_2\text{O})_x^{3+}$ and SO_4^{2-} , presumably after first dissolving the oxide layer. We are not certain if there are any hydroxylated aluminum ions, $\text{Al}(\text{OH})_y^{(3-y)+}$, on the surface. The 2800-3600 cm^{-1} region where the O-H stretch mode would absorb is extremely congested due to the presence of large amounts of water and sulfuric acid on the aluminum surface. It is thus difficult to rule out the formation of a hydroxy complex. However, the presence of H_3O^+ in our IR spectra, even after four hours of exposure, suggests that the adsorbed layer is highly acidic, which may preclude any $\text{Al}(\text{OH})_y^{(3-y)+}$ ion formation. We will discuss this further below.

The changes in the IR spectra observed as a function of water and sulfur trioxide exposure result from reactions occurring on the Al surfaces and not from simple dilution of the sulfuric acid or experimental artifacts. We have performed parallel experiments on Au surfaces, where neither the SO_4^{2-} nor the $\text{Al}(\text{H}_2\text{O})_x^{3+}$ absorption features were ever observed, despite the fact that the weight gain on both Al and Au samples were the same under the same experimental conditions. On Au, we have also observed the deposition of H_2SO_4 , but the IR spectra did not change with time during the entire 240 minute exposure (except that every peak increased in intensity with time). Thus, on Au, sulfuric acid deposits on the metal substrate but does not react with it.

To further confirm the occurrence of corrosion on the Al samples, we have taken *ex-situ* AFM images after a 240 minute exposure to 0.68 Torr SO_3 at 80% RH. The image shown in the left panel of Figure 3 is of a clean Al surface whereas the image in the right panel is of an Al surface after exposure to sulfuric acid. The results indicate that after H_2SO_4 exposure, the Al surface was covered with an $\sim 200\text{\AA}$ thick layer of a solid polycrystalline substance. (Visual



R



L

Figure 3. AFM images of clean (left) and corroded (right) aluminum surfaces. The morphology has changed significantly. The features shown in the right panel are about 200Å high.

examination revealed a mosaic of thin crystals covering the surface). Although *ex situ* AFM measurements may not accurately reflect what occurs during exposure to the gaseous reagents, there is little doubt that a solid salt layer was formed on the surface. Detailed real time *in-situ* AFM studies will be published elsewhere.²³

In summary, we have observed the deposition of sulfuric acid films on aluminum surfaces and their subsequent dissociation and reaction with the metal substrate. We have identified a number of features in the IRAS spectra and used them to delineate the chemistry involved. *Ex-situ* AFM measurements support the occurrence of corrosion.

2.4 Corrosion Rate

2.4.1 Humidity Influence

Varying the relative humidity will influence the corrosion process in two ways. First, the composition of the deposited films is a function of the humidity. Thus, the higher the relative humidity, the more dilute are the acid films. Second, laboratory studies have shown that above a 'critical' relative humidity, corrosion rates sharply increase.²⁴ This 'critical' relative humidity is thought to be related to the vapor pressure above a saturated solution of the salt produced by the corrosion process.³

In order to evaluate the role of relative humidity on the rate of corrosion, we exposed clean Al surfaces to fixed flows of SO₃ (and thus constant sulfuric acid deposition rate) at a partial pressure of 0.68 Torr at 30% and 80% RH. The characteristic infrared absorption of SO₄²⁻ at 1103 cm⁻¹ was used as a measure of the anion concentration and was compared to the absorption from the complementary cation, hydrated Al³⁺, at 2510 cm⁻¹. The growth in the absorption features of both ions is expected to be similar if they arise from the same chemical reaction.

In Figure 4, the time dependence of the peak absorbances of SO₄²⁻ (left panel) and Al(H₂O)_x³⁺ (right panel) are shown, with Curve (a) measured at 80% RH and Curve (b) at 30% RH. In each plot, the absorption of both species initially increased very slowly. The reaction rate appeared to be the same at both low and high humidities. After this initial period (~ 100 minutes), however, significant changes occurred in both spectral regions. At 80% RH, the SO₄²⁻ IR absorbance increased dramatically, whereas at 30% RH, there was no apparent change. The Al(H₂O)_x³⁺ peak increased even more dramatically with time at 80% RH than at 30% RH. Although part of this rapid change in absorption intensity may have been due to changes in the water coordination number, x, of the aluminum ions at each relative humidity (see Discussion), the time dependences of both anion and cation absorbances are qualitatively similar. At 80% RH, the

Growth of Corrosion Product

Effect of Relative Humidity

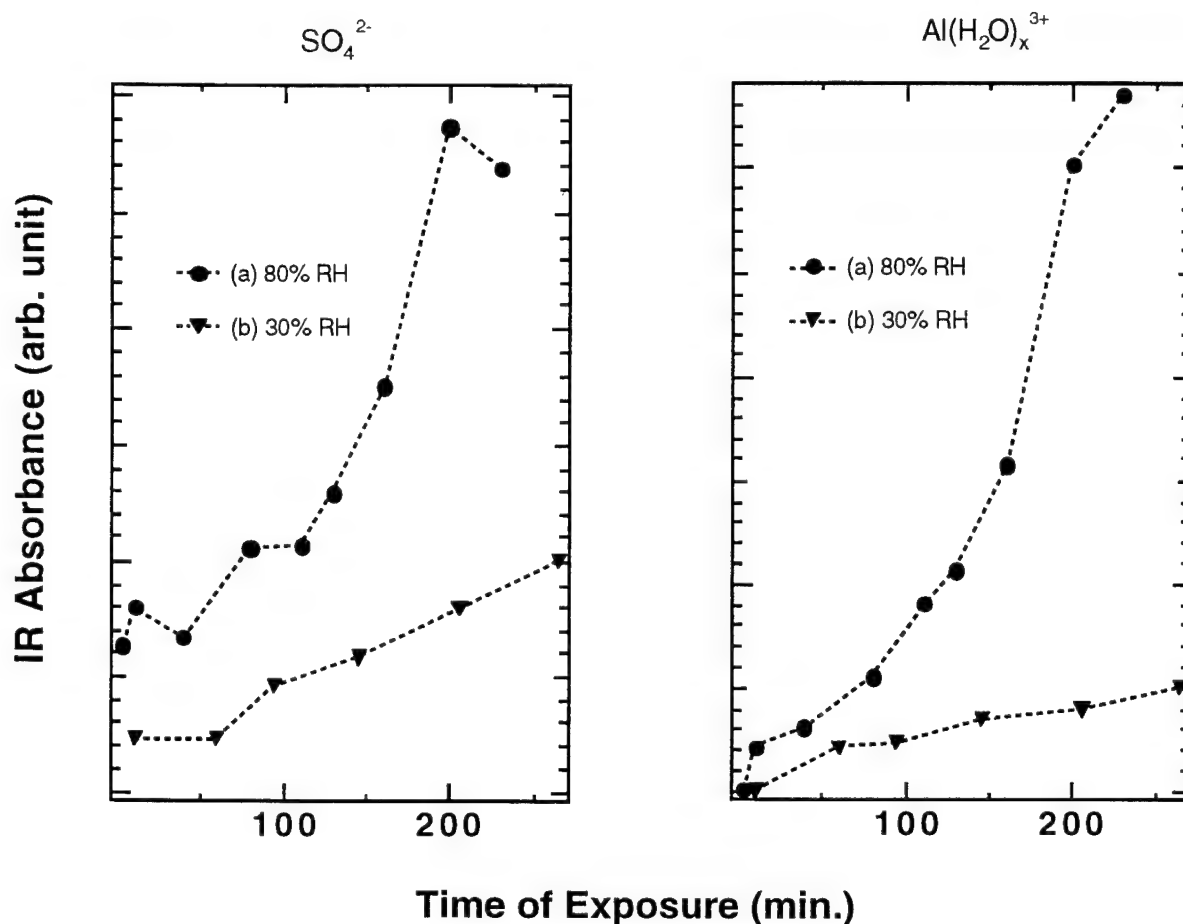


Figure 4. Absorbances of the corrosion products on an Al surface at two different relative humidities as a function of exposure time ($P = 0.68$ Torr). Left panel: SO_4^{2-} IR peak absorbance; right panel: $\text{Al}(\text{H}_2\text{O})_x^{3+}$. (a) 80% relative humidity; (b) 30% relative humidity.

anion and cation absorbances both increased much more rapidly than at 30% RH. This result clearly indicates that the rate of corrosion is significantly enhanced at high relative humidities.

The conclusion that high humidity promotes corrosion is further supported by comparison of IRAS spectra of Al in the $800\text{-}1500\text{ cm}^{-1}$ region at different humidities. Figure 5 presents IRAS spectra of Al after 3 minutes (left panel) and 240 minutes (right panel) exposure to sulfuric acid. Curve (a) was recorded at 80% RH and Curve (b) at 30% RH. After 3 minutes exposure,

IR Spectra on Al

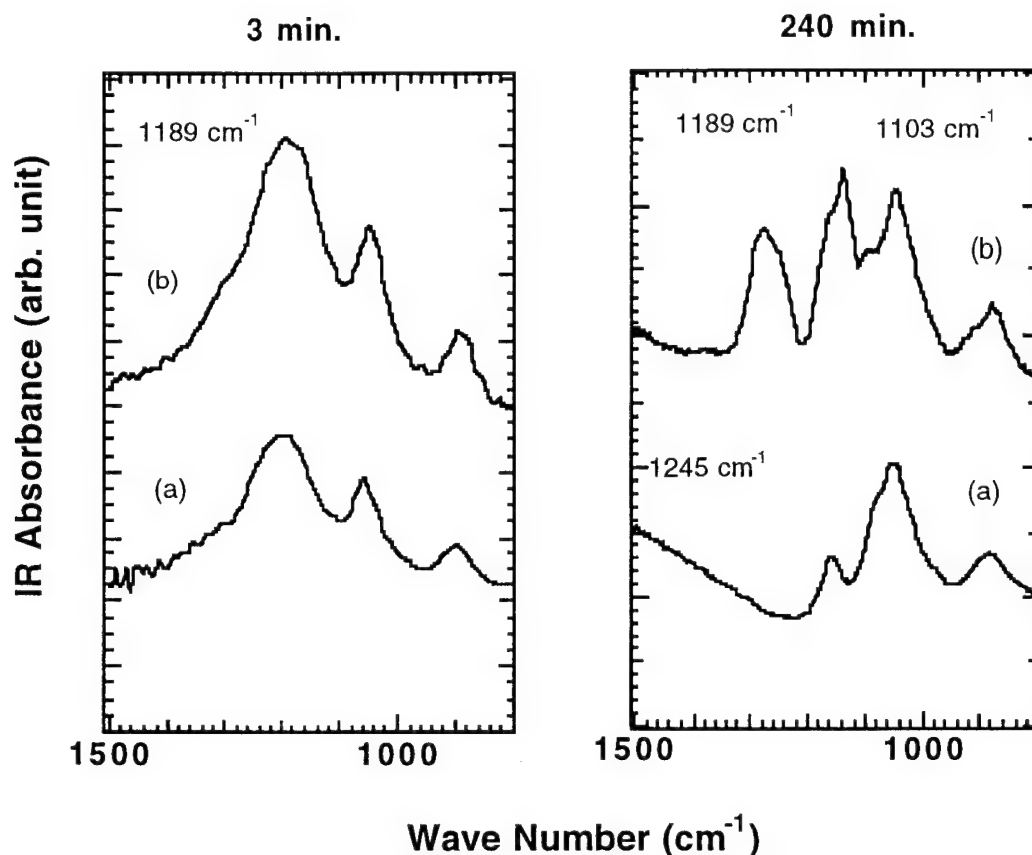


Figure 5. IR spectra of an aluminum surface after 3 minutes (left panel) and 240 minutes (right panel) exposure. $P = 0.68$ Torr and (a) 80% relative humidity and (b) 30% relative humidity.

sulfuric acid is present on the surface at both relative humidities as shown in the left panel. After 240 minutes exposure, though, it is evident that at 30% RH, a large amount of HSO_4^- and unreacted H_2SO_4 remained on the surface, whereas at 80% RH most of the H_2SO_4 was converted to SO_4^{2-} . It can thus be concluded that the reaction efficiency is much lower at 30% RH and that the low corrosion rate is not simply a result of a low supply of H_2SO_4 on the surface. We propose a mechanism in the Discussion section that attempts to explain the observed humidity effect.

2.4.2 Dependence on Initial SO_3 Partial Pressure

The sulfuric acid films grow by the deposition of sulfuric acid droplets that are formed by the reaction of SO_3 with water vapor. At a fixed relative humidity (and thus composition) the rate of sulfuric acid film growth is determined by the initial SO_3 partial pressure. By varying the initial SO_3 concentration, we can extract kinetic information about the corrosion process. Figure 6

Growth of Corrosion Product

Effect of P_{SO_3}

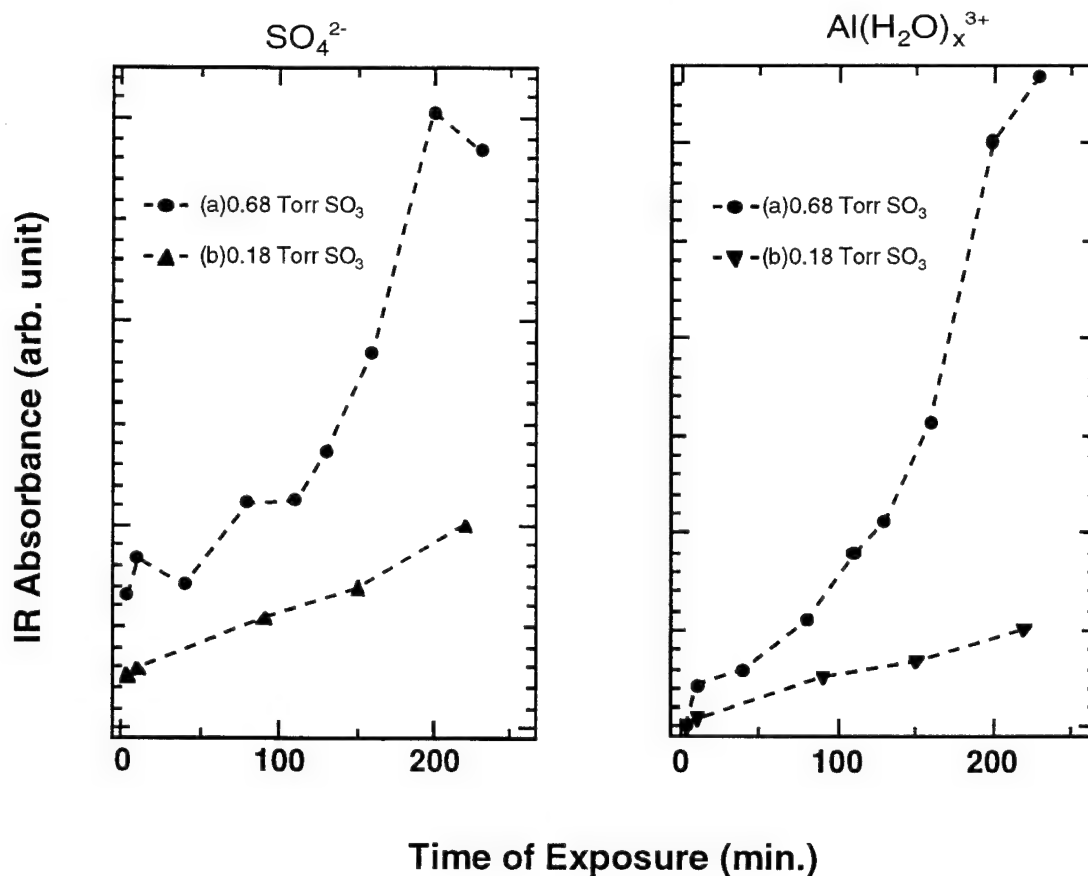


Figure 6. Absorbances of the corrosion products on an Al surface at two different SO_3 partial pressures as a function of exposure time (80% relative humidity). Left panel: SO_4^{2-} ; right panel: $\text{Al}(\text{H}_2\text{O})_x^{3+}$. (a) $P = 0.68$ Torr and (b) $P = 0.18$ Torr.

shows a plot similar to Figure 4, except that the relative humidity is kept at 80%, while the SO_3 partial pressure is varied from 0.68 Torr (Fig. 6(a)) to 0.18 Torr (Fig. 6(b)). The left and right panels present plots of the IR absorbances of SO_4^{2-} (1103 cm^{-1}) and $\text{Al}(\text{H}_2\text{O})_x^{3+}$ (2510 cm^{-1}) respectively as a function of time. Again, both $\text{Al}(\text{H}_2\text{O})_x^{3+}$ and SO_4^{2-} absorbances were found to increase with time. At the same humidity, high SO_3 partial pressure corresponded to higher corrosion rates and more corrosion product, as measured by both the $\text{Al}(\text{H}_2\text{O})_x^{3+}$ and SO_4^{2-} absorbances. This result suggests that at this humidity (and acid composition), the deposition rate of sulfuric acid is the limiting factor in the rate of corrosion.

The above argument is further supported by the spectra shown in Figure 7. Here we present the time evolution of the IR spectra during sulfuric acid exposure, with $P_{\text{SO}_3} = 0.036$ Torr at 80% RH. The IR spectra of aluminum surfaces, shown in Figure 7 (top panel), are quite different from those obtained at high SO_3 partial pressure (Figure 2), where H_2SO_4 was observed on the metal surface at short exposures. At low SO_3 partial pressures, there was no detectable H_2SO_4 on the surface even at short exposure times; instead, only SO_4^{2-} and H_3O^+ species were observed. To prove that this was not simply due to sulfuric acid dilution, we repeated the experiments on Au. On this surface only HSO_4^- and H_2SO_4 are observed at all exposure times [Figure 7 (bottom panel)]. Thus, we can conclude that, under these conditions, the sulfuric acid reacts with the aluminum as fast as it can deposit on the surface.

We have used the infrared absorption features of $\text{Al}(\text{H}_2\text{O})_x^{3+}$ (2510 cm^{-1}) and SO_4^{2-} (1103 cm^{-1}) to measure the relative rates of corrosion. Based on our experimental results, we conclude that high relative humidity promotes corrosion. Within the range of SO_3 partial pressures investigated, the reaction seemed to be limited by sulfuric acid deposition rates at high humidity; at low humidity, there is an excess amount of unconsumed H_2SO_4 on the surface after reaction, indicating that the reaction rate is slower.

2.5 Discussion

Several obvious questions can be raised based on the results presented above. Can relative corrosion rates as a function of humidity be extracted? If so, what are the underlying factors that determine these rates? If a precipitate forms, what is its composition? And does the picture of corrosion that emerges from these results agree with the commonly accepted model presented in the Introduction? We will attempt to address these issues below.

We have presented strong evidence that the products of concentrated sulfuric acid induced corrosion of aluminum surfaces are $\text{Al}(\text{H}_2\text{O})_x^{3+}$ and SO_4^{2-} under the conditions present in these experiments. We have observed significant increases in the concentration of SO_4^{2-} and $\text{Al}(\text{H}_2\text{O})_x^{3+}$ species as a result of corrosion of Al surfaces; on Au, neither sulfate nor hydrated metal cations are observable under identical conditions. Although it is reasonable to assume that $\text{Al}(\text{OH})_y^{(3-y)+}$ species concentrations are extremely low in the highly acidic environment found in these experiments,²⁵ we are unable to confirm this point with our IR spectra because of the broad

Low SO₃ Concentration

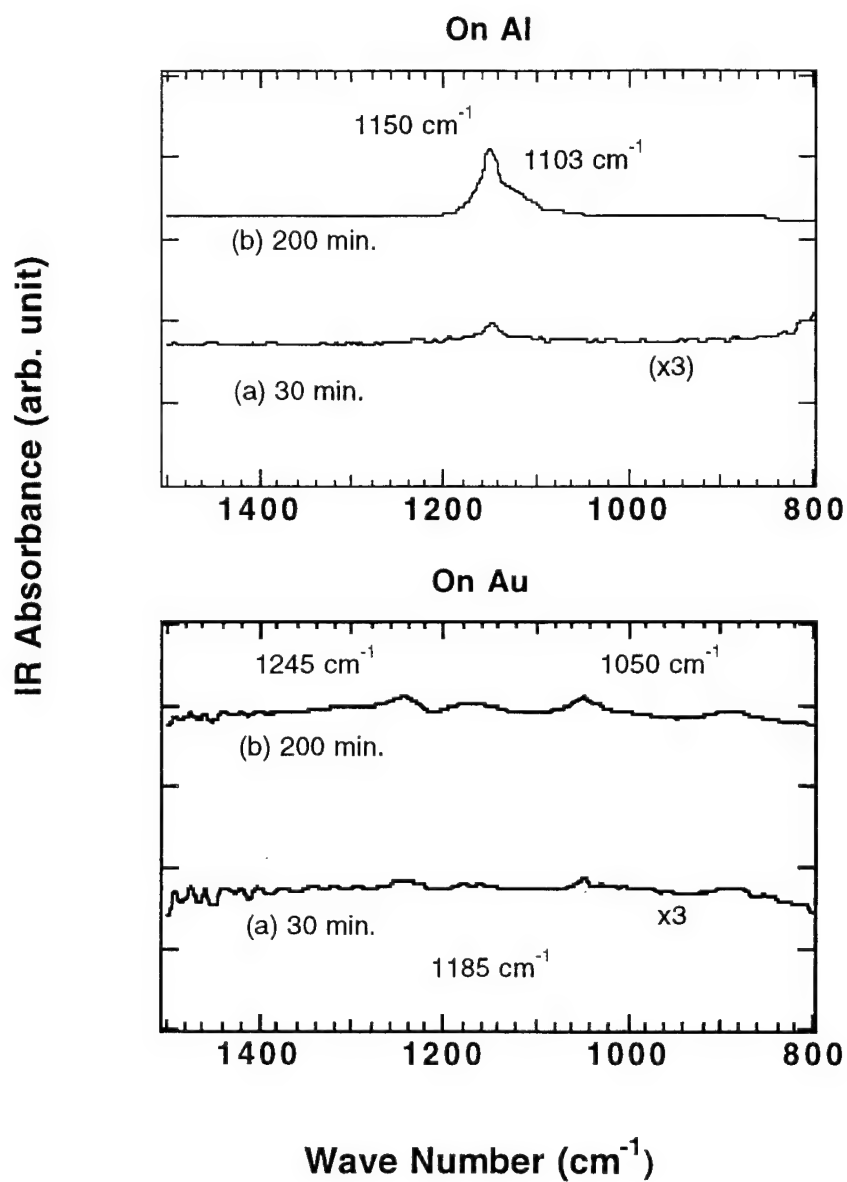


Figure 7. Time evolution of IRAS spectra on Al (top panel) and Au (bottom panel); Exposure: (a) 30 min. and (b) 200 min. $P = 0.036$ Torr and 80% relative humidity.

absorption from H_2O and H_2SO_4 between 2800 and 3600 cm^{-1} . However, a recent study by Tschinkel, et al.²⁶ presents evidence that the O-H stretch in the $\text{Fe}(\text{OH})_y$ species appears as a sharp feature above 3600 cm^{-1} . We have not seen such a feature. Based on our findings, we presume that any precipitates that form are hydrated aluminum sulfate and not hydroxysulfate salts.

Based on our results, we believe that the increase in IR absorbance of SO_4^{2-} provides a good measure of the corrosion product. We can use the data presented in Figure 4 and Figure 6 to derive a phenomenological corrosion rate constant, k , at 80% and 30% RH. This rate constant is defined as the slope of SO_4^{2-} IR absorbance versus time, since the reaction order is not known. For the first 100 minutes, the growth rate of the sulfate peak was the same at both humidities. After about 100 minutes, we noticed a dramatic difference between the two different humidities. In this latter time region, the ratio of the corrosion rates is approximately:

$$\frac{k_{(80\% \text{ rel. hum.})}}{k_{(30\% \text{ rel. hum.})}} \approx 5 \pm 2$$

If we use the 2510 cm^{-1} peak $[\text{Al}(\text{H}_2\text{O})_x^{3+}]$ as a measure of corrosion, the difference is even more dramatic. The discrepancy in the apparent ratio of corrosion rates may simply be due to an increase in the water coordination number, x , of the hydrated aluminum ion at the higher relative humidity. Qualitatively speaking, though, the SO_4^{2-} and $\text{Al}(\text{H}_2\text{O})_x^{3+}$ measurements agree. This result is consistent with the concept of 'critical' relative humidity.

An important issue is the dramatic increase in corrosion rates when the relative humidity was raised. Based on the calculations of Carslaw et al.,¹⁹ the activities of both bisulfate and hydronium ion in pure sulfuric acid decrease by a factor of three as the relative humidity is raised from 30% to 80%. One might therefore argue that corrosion should decrease as humidity is increased; yet the observed corrosion rate increases by a factor of ~5. Although the activities of these species are probably strongly perturbed by the presence of aluminum cations, it is clear that simple arguments along these lines will not provide an answer.

Insight into the mechanisms underlying the humidity effect on corrosion rates is provided by *in situ* real time AFM studies of sulfuric acid induced corrosion of Al surfaces to be reported elsewhere.²³ The most striking result of these experiments is that when the relative humidity is maintained below 30%, a solid salt appears to be a major corrosion product. As the relative humidity is raised above 75%, the salt absorbs water and becomes more fluid. Graedel has listed over 25 hydrated aluminum sulfate and hydroxy-sulfate salts that might form naturally.³ These include both crystalline forms and metastable amorphous salts as well. Based on these

observations, we can speculate that the large increase in corrosion rate at high humidities is related to hydration of the precipitation layer.

At low humidity, once reaction occurs, a layer of solid salt forms between the sulfuric acid and the Al substrate as a result of the corrosion process. This salt layer inhibits attack on the substrate by sulfuric acid by acting as a permeation barrier. At higher relative humidities, however, the picture is different. The corrosion product, aluminum sulfate, takes up water and becomes quite permeable to diffusion of the sulfuric acid layer to the substrate. Once H_2SO_4 reaches the metal/salt interface, more corrosion can occur. This mechanism is further supported by our IR studies. We have shown that after 240 minutes at 80% RH almost no sulfuric acid was left on the surface, whereas at 30% RH, a significant amount of H_2SO_4 remained on the surface. We also observed a much more dramatic increase in the water peak absorption at 2510 cm^{-1} compared to the sulfate peak absorption at high relative humidities. This absorption arises from water coordinated to Al^{3+} . Together with our AFM observations, these results suggest that as the humidity is raised, the water coordination number and concentration of this particular corrosion product increases. Unfortunately due to the limited amount of data, we cannot quantify this point.

From the results discussed above, we can now present a clearer picture of the chemical processes underlying sulfuric acid-induced corrosion of aluminum. First, a sulfuric acid film will form with a composition determined by the relative humidity and substrate temperature and at a rate determined by the concentration of the acid precursor species (in this case SO_3). At a sufficiently low pH, the protective metal oxide layer will dissolve and the underlying metal will undergo acid-promoted oxidation to form aluminum cations. The chemical composition of the corrosion layer will reflect this process. The observed composition is the product of a competition between sulfuric acid deposition and the corrosion process, which involves reaction of hydronium ion with the metal and consequent dissociation of the sulfuric acid. At high humidities and low SO_3 concentrations, the corrosion rate is sufficiently high to prevent the buildup of any sulfuric acid. At sufficiently high cation concentrations, aluminum sulfate salts will precipitate and, under low humidity conditions (below the 'critical' relative humidity), inhibit further corrosion.

We are now beginning experiments using sulfur dioxide and hydrogen peroxide as precursor gases to sulfuric acid formation. Any interpretation of these studies will be complicated by the need to understand the aqueous uptake of hydrogen peroxide vapor and its subsequent role in the oxidation of sulfur dioxide. Preliminary results indicate that concentrated sulfuric acid films can be formed on aluminum in this fashion.

2.6 Conclusions

In this paper, we have shown that when sulfuric acid deposits on a room temperature Al surface, corrosion occurs and hydrated aluminum sulfate is the principle of the product. The corrosion rate is very sensitive to the relative humidity and deposition rate of sulfuric acid. High humidity promotes corrosion. We believe that this observation is related to the phase of the corrosion product. At low humidity, aluminum sulfate is more solid-like and acts as a barrier between the sulfuric acid and the metal surface, inhibiting corrosion. As the humidity increases, the precipitate takes up water, becoming permeable to acid diffusion to the surface. Although the ratio of the water to SO_3 partial pressures in these experiments ranges from 10:1 to 400:1, concentrated sulfuric acid films are formed because of a quasi-equilibrium established between the water vapor and the adsorbed acid film. This result indicates that if there is no strong competition from chemical reaction, the acid concentration on surfaces can be quite high, depending on the relative humidity. Thus, although initial acid deposition from acid rain, dew and fog produces films in the pH range of 2-4, subsequent wetting and drying cycles may produce highly acidic environments similar to those established in these experiments.

2.7 Acknowledgments

This research was conducted with financial support from the Air Force Office of Scientific Research under the Small Business Innovation Research program. Miquel Salmeron of Lawrence Berkeley Laboratory is gratefully acknowledged for providing access to an atomic force microscope. Daniel Oblas of the University of Massachusetts Lowell Center for Advanced Materials is also acknowledged for obtaining the ex situ XPS measurements of the corroded aluminum sample. The authors thank John Jayne for the preparation of the sulfur trioxide sample, J. B. McManus for the design and construction of the optical bench, and Douglas Worsnop and Charles Kolb for many useful discussions regarding sulfuric acid formation and chemistry. They also thank Thomas Graedel for offering invaluable insights into atmospheric corrosion chemistry.

2.8 References

1. V. Kucera and E. Mattson, in *Corrosion Mechanisms*, Marcel Decker, New York (1987), F. Mansfeld, Editor, p. 211.
2. E. Mattsson, *Basic Corrosion Technology for Scientists and Engineers*, Wiley, New York (1989)
3. T.E. Graedel, *J. Electrochem. Soc.* **136**, 204C (1989).
4. T.E. Graedel, *Mat. Res. Soc. Symp. Proc.* **125**, 95 (1988)

5. P. Wayne, *Chemistry of Atmospheres*, 2nd ed. (Oxford, 1991), p. 244.
6. J.J. Friel, *Corrosion* **42**, 422 (1986).
7. H. Bassett and T.H. Goodwin, *J. Chem. Soc.* **2239** (1949).
8. R.T. Foley and T.H. Nguyen, *J. Electrochem. Soc.* **129**, 464 (1982)
9. J. Pritchard, *Chemical Physics of Solids and their Surfaces*, Vol. 7, M.W. Roberts and J.M. Thomas, eds. (Chemical Society, London, 1977).
10. R.M. Crooks, C. Xu, L. Sun, S.L. Hill, and A.J. Ricco, *Spectroscopy* **8**, 28 (1993)
11. Y. Chabal, *Surf. Sci. Reports* **8**, 211 (1988)
12. D. Persson and C. Leygraf, *J. Electrochem.* **140**, 1256 (1993)
13. S. Dushman, *Scientific Foundations of Vacuum Technique*, 2nd Edition, New York, Wiley, 1962
14. *Handbook of Chemistry and Physics*, CRC Press (Boca Raton, 1990) D.R. Lide, Editor, page 6-53.
15. E.E. Ferguson, F.S. Fehsenfeld and A.L. Schmeltkopf, *Adv. At. Mol. Phys.* **5**, 1 (1969)
16. C.E. Kolb, J.T. Jayne, D.R. Worsnop, M.J. Molina, R.F. Meads and A.A. Viggiano, *J. Am. Chem. Soc.* **116**, 10315 (1994)
17. L. Volpe, in *Proceedings of the 10th International Congress on Metallic Corrosion*, Madras, India (Nov. 1987), p. 4091.
18. M.R. Querry, R.C. Waring, W.E. Jolland, L.M. Earls, M.D. Herrman, W.P. Nijm and G.M. Hale, *J. Opt. Soc. Am.* **64**, 39 (1974)
19. K.S. Carslaw, S.L. Clegg, and P. Brimblecombe, *J. Phys. Chem.*, submitted for publication
20. R. Zhang, P.J. Woolridge, J.P. Abbat and M.J. Molina, *J. Phys. Chem.* **97**, 7351 (1993)
21. A.M. Middlebrook, L.T. Iraci, L.S. McNeill, B.G. Koehler, M.A. Wilson, O.W. Saastad and M.A. Tolbert, *J. Geophys. Res.* **98**, 473 (1993)
22. J.F. McIntyre, R.T. Foley, and B.F. Brown, *Appl. Spectrosc.* **36**, 128 (1982)
23. Manuscript in preparation.
24. A. Bukowiecki, *Schweiz. Arch.* **32**, 42 (1966)
25. F.A. Albert and G. Wilkinson, *Advanced Inorganic Chemistry*, 3rd Edition, Wiley, New York, 1972
26. W. Tschinkel, H. Neugebauer and A. Neckel, *J. Electrochem. Soc.* **137**, 1474 (1974)

3. EX SITU IRAS MEASUREMENTS ON CORRODED ALUMINUM SAMPLES

The following section is divided into several parts describing the experimental tests performed in order to demonstrate the feasibility of using the IRAS technique to detect incipient corrosion on metal samples. In addition to performing IRAS measurements, we have also taken x-ray photoelectron spectra (XPS) and atomic force micrographs in order to provide corroborative evidence as to chemical composition and morphology of the corroded samples. First, we describe the experimental techniques involved and then present the results, followed by a brief discussion.

We have performed corrosion measurements on two types of aluminum samples. The first are cut from 0.25 mm thick aluminum foil (Aesar, 99.997% purity) and have surface defects that are noticeable to the eye (labeled rough). The second are cut from silicon wafers on which aluminum has been vapor deposited. These samples have a mirror finish and have an average surface roughness of less than 20 Å (labeled smooth). In order to simulate the corrosive action of a typical rainfall cycle, both types of samples were sprayed with a sulfate solution having a pH of 3.5. The samples were then placed in a glovebag with a beaker of water to provide high humidity and kept in an oven at 38 °C (100 °F) for one day. Half the samples were then resprayed with the sulfate solution and exposed to high humidity for a second day. A set of reference samples were kept out in room air for the entire period. All corroded samples were noticeably mottled in appearance, with the less corroded samples having a lower density of spots.

3.1 IRAS Measurements

The IRAS measurements were performed on a Perkin-Elmer FTIR spectrometer in the Center for Advanced Materials at the University of Massachusetts-Lowell. The incidence angle of the infrared beam was 60 degrees off normal and the detector was a DTGS detector providing coverage from 400 cm^{-1} to 4000 cm^{-1} . All the spectra shown are transmission spectra referenced to non-corroded surfaces. Figure 1 shows IRAS spectra from 400-4000 cm^{-1} of the less and more corroded samples for the smooth aluminum. The corroded samples reflect a lower fraction of the incident light than the native samples. Prominent absorption features indicative of corrosion formation are noticeable in all the spectra. These results are strikingly similar to those recorded in the flow cell experiments reported in the previous section. Figures 2 and 3 show higher resolution spectra in the 3100 cm^{-1} and 1000 cm^{-1} regions. What becomes apparent is that the absorption peak at 2510 cm^{-1} which we have assigned to the presence of hydrated aluminum ions (either aqueous or in a salt) is indicative of the corrosion process.

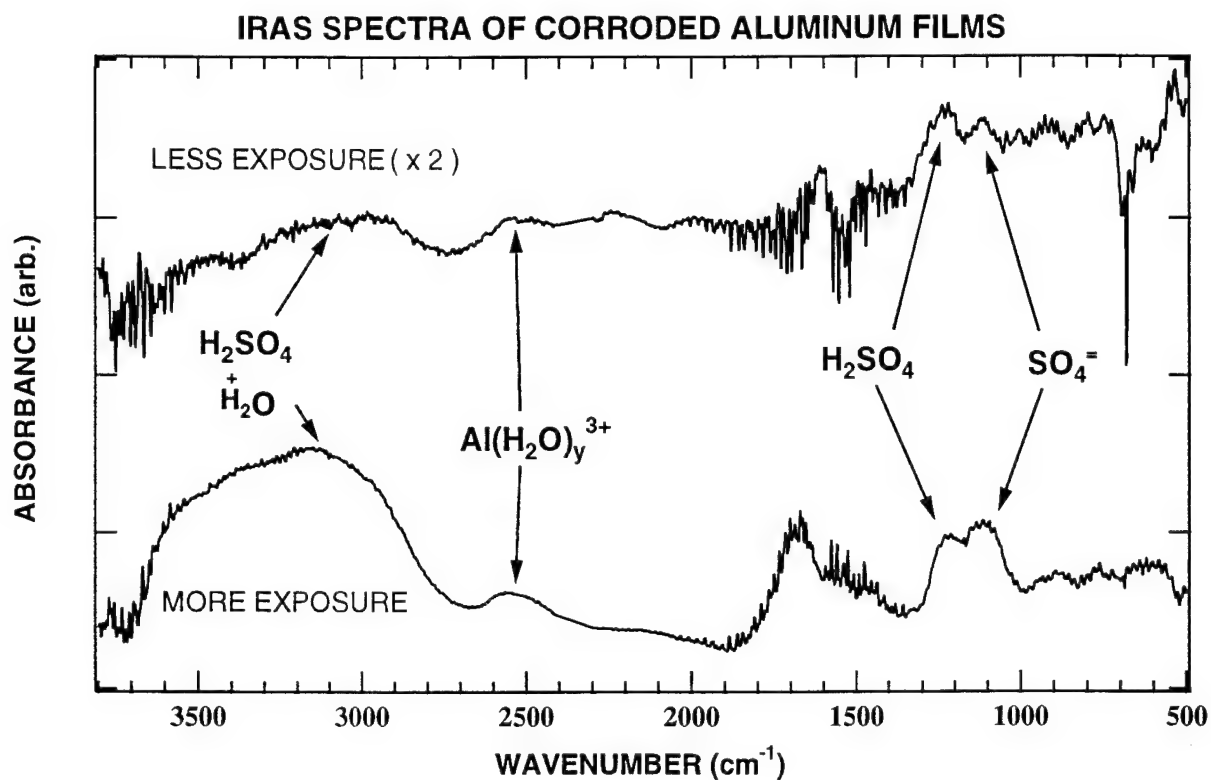


Figure 1. Infrared Reflection Absorption Spectrum (IRAS) of corroded smooth aluminum samples which were exposed to acidic sulfate solution and high humidity.

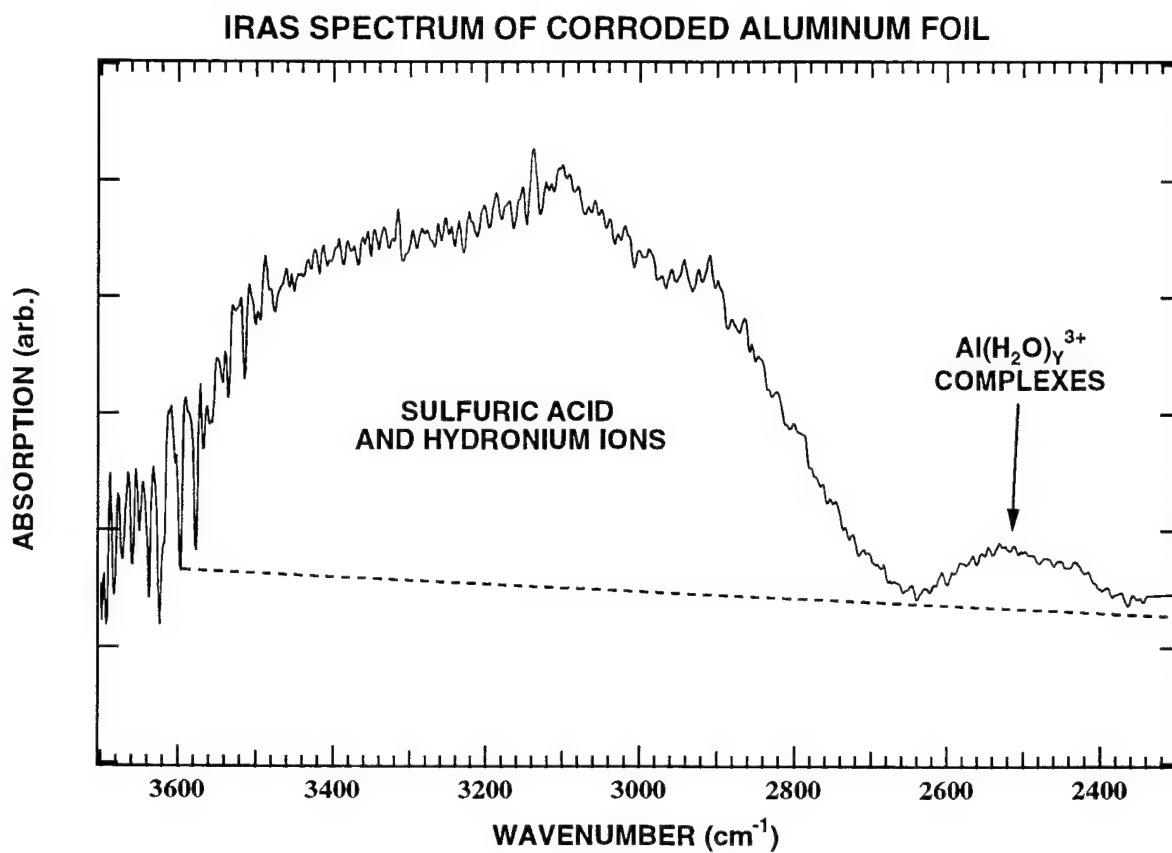


Figure 2. High resolution IRAS spectrum of 3100 cm⁻¹ region for a corroded rough aluminum foil sample

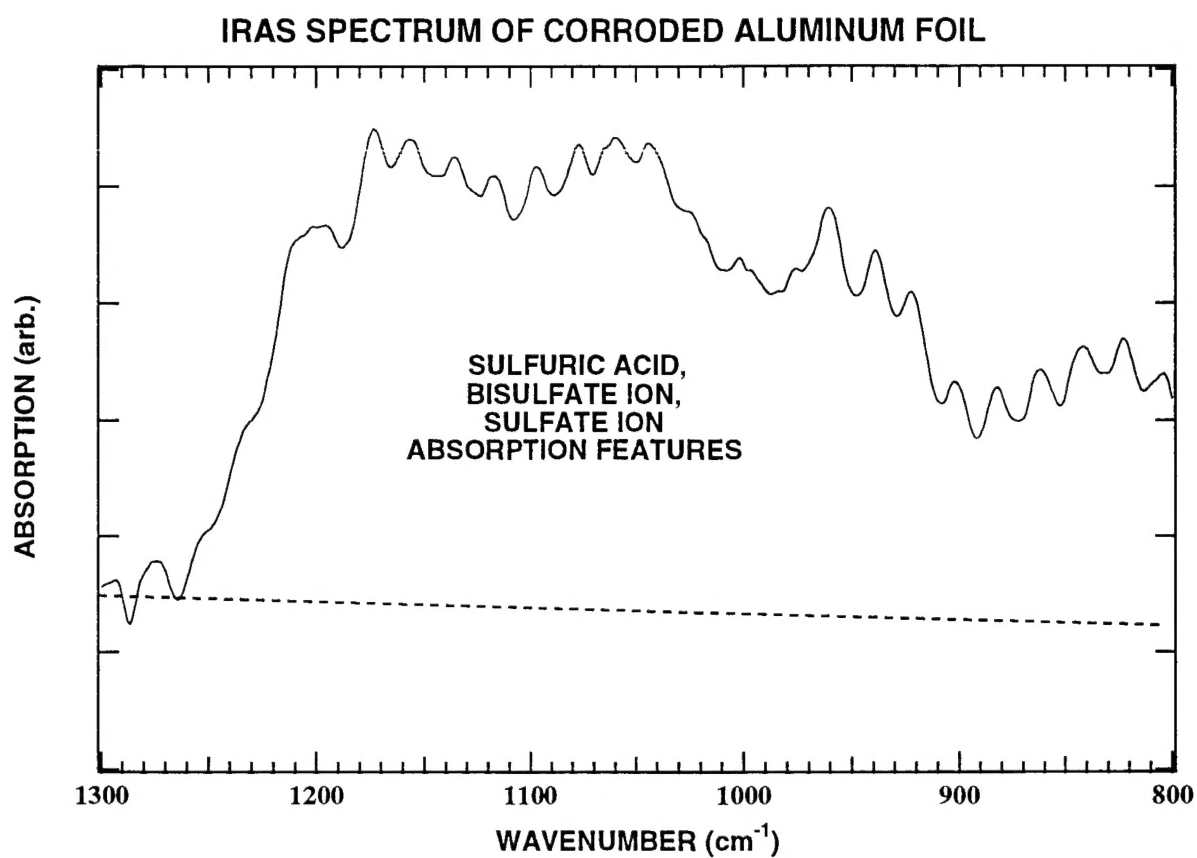


Figure 3. High resolution IRAS spectrum of 1100 cm⁻¹ region for a corroded rough aluminum foil sample

3.2 X-ray Photoelectron Spectroscopy (XPS)

In order to check the chemical composition of the corroded films and obtain an estimate of the depth of the etch pits, high resolution XPS spectra were measured on an ESCALAB II instrument (Fisons) using a Mg cathode and a bandpass energy of 20 eV. Figure 4 presents a representative aluminum spectrum for a corroded foil and a clean reference sample. The reference spectrum shows both metallic aluminum and an aluminum oxide layer which is no more than 50 Å thick. After exposure to the dilute sulfuric acid solution, the oxide peak is considerably broadened and much of the oxide layer has been converted to another species. Deconvolution of this peak indicates the formation of a more highly oxidized form of aluminum, probably aluminum sulfate. The sulfur XPS peak indicates that the sulfur is in the sulfate form. It should be stressed that our ability to observe any metallic aluminum in the corroded sample XPS spectrum indicates that on the average, the corrosion film is no more than 50-60 Å thick (based on known electron escape depths), even though locally it is probably much higher (see paragraph below on AFM images).

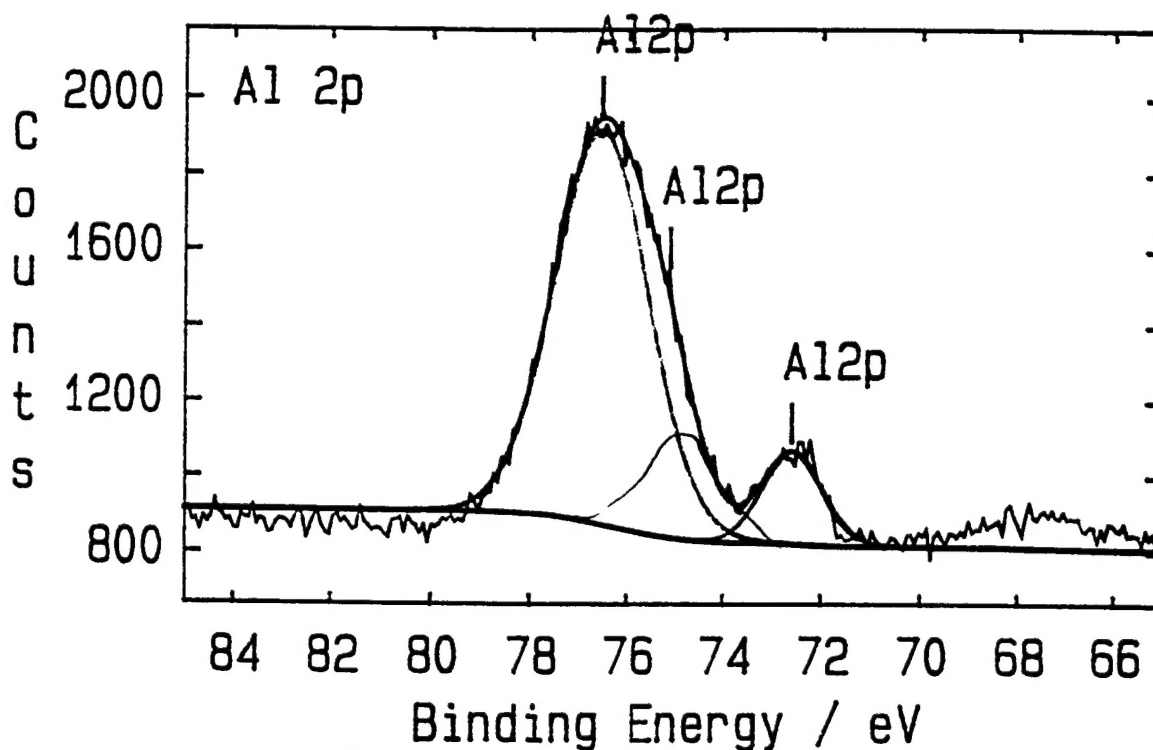


Figure 4. XPS spectrum of the aluminum 2p peak for a corroded rough aluminum foil sample.

3.3 Atomic Force Microscopy

Atomic force micrographs (AFM) were obtained on a Park Scientific Instruments SFM-BD2 atomic microprobe on the smooth samples in order to check the morphology. Measurements on the less corroded samples showed bumps that were $\sim 1\ \mu\text{m}$ in diameter and $500\ \text{\AA}$ high. The more corroded samples showed bumps that were twice as wide and high and with a much higher density. Figure 5 shows a micrograph ($20\ \mu\text{m} \times 20\ \mu\text{m}$ scale) of the less corroded sample. The formation of bumps are probably due to the formation of hygroscopic aluminum salts. Even after ultrasonic water bath cleaning, the bumps are still observable even though some of the corrosion layer has been removed. These observations are consistent with a corrosion mechanism where chemical attack takes place at a surface crack or defect and then spreads. Visual evidence indicates that the rougher foil samples were more rapidly attacked than the smooth substrates.

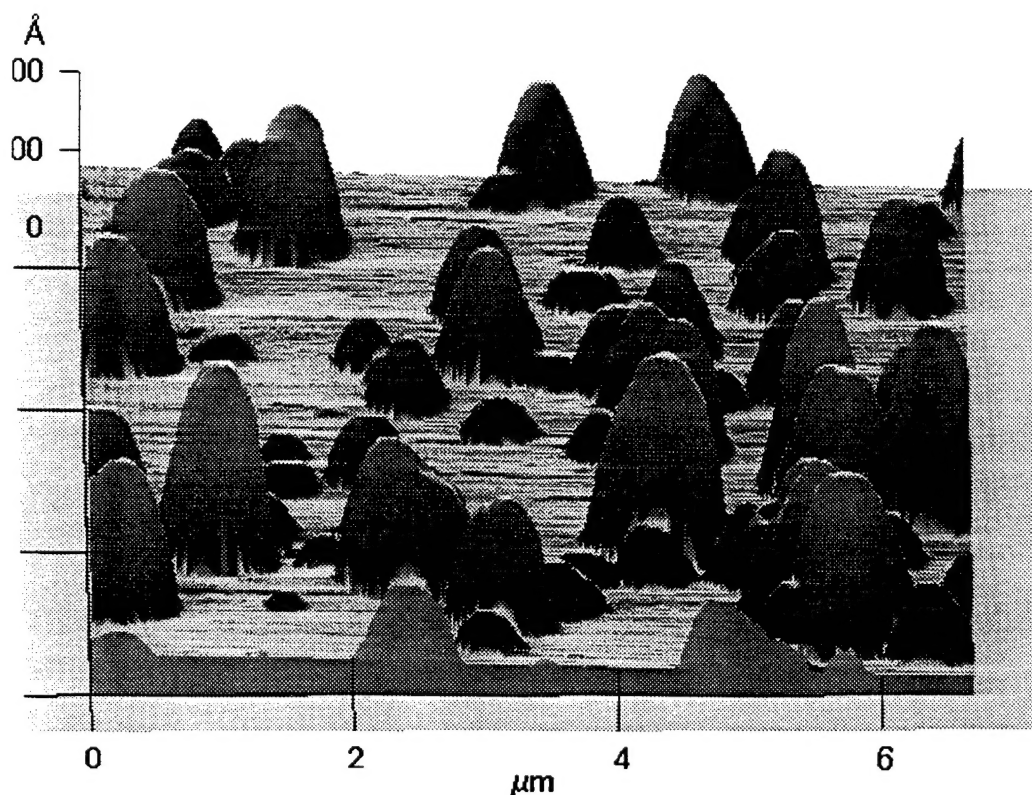


Figure 5. Atomic force micrograph of corroded smooth aluminum sample.

3.4 Discussion

We have demonstrated that the IRAS technique provides unequivocal detection of metal corrosion at the sub-micron level. Moreover, an ambiguous absorption peak at 2510 cm^{-1} , which is directly related to the presence of corroded aluminum, is in a spectral region not affected by the absorption by atmospheric water and carbon dioxide. This greatly simplifies the design of a depot-level monitor since it may not be necessary to use nitrogen purging or polarization modulation techniques to observe corrosion induced absorption features. The assignment of the IRAS spectrum is strengthened by the corroborating evidence presented in the XPS and AFM data. We have definitely formed a reaction layer than contains aluminum sulfate and it has physically perturbed the aluminum surface. Thus, we can rule out the possibility that all we have observed is the condensation of a concentrated sulfuric acid solution.

All of the data presented above is in agreement with the corrosion literature. (See V. Kucera and E. Mattson in "Corrosion Mechanisms", Dekker Inc., New York, 1987, F. Mansfield, ed., pgs. 211-284, for an excellent discussion of atmospheric corrosion.) The chemical action of sulfate ions at low pH in a humid atmosphere leads to the removal of the protective oxide layer, followed by oxidation of aluminum metal to ions. The result is the formation of a hygroscopic reaction layer of aluminum sulfate and hydroxysulfate salts, some of which are insoluble. Ultrasonic cleaning of corroded samples for two days did not remove much of the corrosion layer. The AFM data indicates that, as expected, corrosion begins at structural defect points on the surface and spreads laterally.